Journal of Geophysical Research: Space Physics

RESEARCH ARTICLE
10.1029/2018JA026011

On Ionic Contributions to Pedersen Conductance

Bruno S. Zossi[1,2], Mariano Fagre[2,3], and Ana G. Elias[1,2]

[1]Laboratorio de Fisica de la Atmosfera, INFINOA (CONICET-UNT), Facultad de Ciencias Exactas y Tecnologia, Universidad Nacional de Tucuman, Tucuman, Argentina, [2]Consejo Nacional de Investigaciones Cientificas y Tecnicas, CONICET, Tucuman, Argentina, [3]Laboratorio de Telecomunicaciones, Departamento de Electricidad, Electrónica y Computación, Facultad de Ciencias Exactas y Tecnología, Universidad Nacional de Tucuman, Tucuman, Argentina

Key Points:
- The relative contribution of each ion spicies to Pedersen conductance is variable
- Atomic oxygen is the main conducting ion near of magnetic field minimum and with high solar activity
- Molecular oxygen contribution to conductance is maximum near of geomagnetic poles

Correspondence to:
B. S. Zossi,
brunozossi@hotmail.com

Citation:
Zossi, B. S., Fagre, M., & Elias, A. G. (2018). On ionic contributions to Pedersen conductance. *Journal of Geophysical Research: Space Physics*, *123*, 10,310–10,318. https://doi.org/10.1029/2018JA026011

Received 17 AUG 2018
Accepted 30 NOV 2018
Accepted article online 8 DEC 2018
Published online 21 DEC 2018

Abstract Ionospheric conductivity is a key parameter to understand the upper atmosphere electrodynamics, magnetosphere-ionosphere-thermosphere coupling and several geophysical processes. In the case of Pedersen conductivity, ions and electrons are moving in opposite direction, so that it results from the addition of the separate contributions. In this work, the role of the three main ions, that is, NO^+, O_2^+, and O^+, in the conductivity height profile and in the conductance global pattern is analyzed for different solar activity levels and seasons. NO^+ is the is the main contributor for the maximum conductivity in all the cases in the *E* layer; however, O^+ takes relevance with a significant percentage of the conductance at certain regions such as the South Atlantic Anomaly and the crests at the equatorial ionization anomaly, becoming the main conducting ion in these zones when the solar activity is high. Regarding seasonal effects, the role of NO^+ in the conductivity is maximum on summer hemisphere, while O^+ becomes important in winter and maximum with high solar activity. O_2^+ has maximum percentage close to magnetic poles, where the magnetic field strength is intense lowering the peak conducting level.

1. Introduction

In a conducting medium, as it is the case of the ionosphere, the conductivity σ is a tensor, whose nature is determined at the microscopic level of the system, which relates an electric current density *J* to an applied electric field *E* through the Ohm's law

$$J = \sigma E \tag{1}$$

In the presence of the Earth's magnetic field, which makes the ionospheric conductivity an anisotropic quantity, equation (1) becomes

$$J = \sigma (E + V \times B) = \sigma E' \tag{2}$$

known as the generalized Ohm's law, where *V* is the neutrals' velocity at which charged particles in the ionosphere are dragged and E' is the effective electric field.

If $E = (E_x, E_y, E_z)$ and *B* along the *z* direction, and considering ions' and electrons' equation of motions in the ionosphere (see, e.g., Rishbeth & Garriott, 1969; Schunk & Nagy, 2009), equation (2) can be written as

$$J = \begin{pmatrix} \sigma_1 & -\sigma_2 & 0 \\ \sigma_2 & \sigma_1 & 0 \\ 0 & 0 & \sigma_o \end{pmatrix} \begin{pmatrix} E_x - V_{ny}B \\ E_x + V_{ny}B \\ E_z \end{pmatrix} = \sigma_1 E'_{\perp} + \sigma_2 \frac{B \times E'}{B} + \sigma_o E_z \tag{3}$$

where σ_1 and σ_2 are the Pedersen and Hall conductivities, respectively, oriented perpendicular to the background magnetic field. σ_o is called the parallel conductivity oriented along the magnetic field line and corresponds to the classical conductivity in the absence of magnetic field. $E'_{\perp}$ is the component of E' perpendicular to *B*, and E_z is the component of *E* along *B*. Each conductivity is given by (Moen & Brekke, 1990; Rishbeth & Garriott, 1969; Takeda & Araki, 1985)

$$\sigma_0 = N_e e^2 \left[\frac{1}{m_e \nu_e} + \Sigma_i \frac{f_i}{m_i \nu_i} \right] \tag{4}$$

$$\sigma_1 = N_e e^2 \left[\frac{1}{m_e} \cdot \frac{\nu_e}{(\nu_{e^2} + \omega_{e^2})} + \Sigma_i \frac{f_i}{m_i} \cdot \frac{\nu_i}{(\nu_{i^2} + \omega_{i^2})} \right] \tag{5}$$

$$\sigma_2 = N_e e^2 \left[\frac{1}{m_e} \cdot \frac{\omega_e}{(\nu_{e^2} + \omega_{e^2})} - \Sigma_i \frac{f_i}{m_i} \cdot \frac{\omega_i}{(\nu_{i^2} + \omega_{i^2})} \right] \quad (6)$$

where subscripts e and i stand for electron and ion respectively, N_e is the electron density, m the mass, e the electron charge, ν the collision frequency, $\omega = eB/m$ the gyrofrequency, B the Earth's magnetic field intensity, and f the relative density of each ion species. Plasma neutrality and single positive charged ion species are assumed. Note that replacing the gyrofrequency in equation (5), a dependency with B^{-2} is obtained.

Collision frequencies of electrons and ions are given by

$$\nu_e = \nu_{en} + \nu_{ei} \quad (7)$$

$$\nu_i = \nu_{in} + \nu_{ie} \quad (8)$$

where ν_{en} and ν_{ei} are the electron-neutral and electron-ion collision frequencies respectively, and the same applies to ion collision frequencies. In the ionosphere at heights where the conductivity is significant, $\nu_{en} \gg \nu_{ei}$ and $\nu_{in} \gg \nu_{ie}$, so $\nu_e = \nu_{en}$ and $\nu_i = \nu_{in}$ is usually assumed.

In particular, Pedersen conductivity maximum occurs near 120 km where ions collision frequency and gyrofrequencies are similar, allowing all ions to travel along $E'_{\perp}$ and electrons along $E' \times B$ with a much smaller contribution to this conductivity. However, each ionic component of σ_1 contributes in different amounts to the total conductivity according to the height level considered, and their corresponding peak values occurs at different heights as well. Consequently, Pedersen conductance, Σ_1, that is the height integrated conductivities given by

$$\Sigma_1 = \int_{z_1}^{z_2} \sigma_1 \, dz \quad (9)$$

where z_1 and z_2 are the bottom and top of the ionosphere, respectively, presents different contributions from each conducting ion type.

The conductivity cannot be measured, but it is indirectly calculated from electron density profile (Brekke et al., 1974; Moen & Brekke, 1993; Robinson & Vondrak, 1984). The solar radiation is the main contributor to ionization, many works has been focused on high latitudes where the conductivity is proportional to Joule heating (Thayer et al., 1995; Strangeway, 2012). Rasmussen et al. (1988) determined theoretical relations between solar radiation and conductivity at high latitudes and was measured by Brekke et al. (1974), Robinson and Vondrak (1984), and Moen and Brekke (1993).

In the present work the contribution of the main ion species to Pedersen conductivity and conductance, and its variation with season and solar activity level are analyzed. The principal ions in the ionosphere are NO^+, O_2^+, and O^+, with neglecting amounts of N_2^+ and N^+. In the upper ionosphere H^+ and He^+ appear but this region does not contribute significantly to Pedersen conductance due to collision frequencies much lower than the gyrofrequency.

There are not many works with this approach, where the conductivity is calculated as the sum of its components. Some articles such as Sheng et al. (2017) calculate the conductance relation of layer *E* to layer *F* in order of estimate the coupling between these layers on different solar and geomagnetic activity scenarios. This work can be compared with the present analysis since *F* layer conductivity is almost completely due to atomic oxygen ion, and *E* layer is the contribution of molecular oxygen and nitric oxide ions.

2. Methodology

Pedersen conductivity height profile and conductance of each ion species separately was estimated according to

$$\sigma_{1i} = \frac{N_i \, e^2}{m_i} \cdot \frac{\nu_i}{(\nu_{i^2} + \omega_{i^2})} \quad (10)$$

and

$$\Sigma_{1i} = \int_{z_1}^{z_2} \sigma_{1i} \, dz \quad (11)$$

where $N_i = N_e f_i$ is the number density of ion i, which stands for NO^+, O_2^+, and O^+. The spatial structure of Σ_1 was assessed on a grid with 5° latitude and 10° longitude resolution, for 12 LT.

Equations (9) was numerically integrated using the trapezoid rule with a simple computer model, that is

$$\int_{z_1}^{z_2}\sigma dz = \Sigma\frac{\sigma(z_{i-1})+\sigma(z_i)}{2}\Delta z \tag{12}$$

where z_1 and z_2 were set to 80 and 400 km, respectively, and Δz to 5 km (smaller height steps do not change significantly the results).

The ion species considered for conductivities assessment are, as already mentioned, the three most abundant at the height range 80–400 km, that is, NO^+, O^+, and O_2^+. Each of them and electrons were assumed to collide with O_2, O, and N_2 that are the most abundant neutral components at the heights here involved. The parameters needed to assess the different collision frequencies are the temperatures of electrons and ions, Te and Ti, the neutral concentrations of O_2, O and N_2, and Ne.

Collision frequencies for each type of collision were calculated from the equations used by the Thermosphere Ionosphere Electrodynamic General Circulation Model (HAO, 2017; Schunk & Nagy, 2009). The variables f_i for each ions species, Ne, and temperatures were obtained from the International Reference Ionosphere, IRI-2012, (Bilitza et al., 2014), while neutral components' densities from the NRLMSISE-00 empirical atmospheric model (Picone et al., 2002). The magnetic field was obtained from IGRF12 (Thebault et al., 2015).

To study solar activity and seasonal effects, we analyzed maximum and minimum solar activity level (years 2001 and 2008) and 3 months: December, July, and March. The dates used in the calculations are the first International Quiet Day of each month: 15 March, 28 July, and 9 December for 2001, and 7 March, 19 July, and 1 December for 2008.

3. Results and Discussion

Figure 1 shows σ_1 height profile for different seasons and solar activity levels. The total conductivity peak height occurs where $\nu_i \approx \omega_i$, that is ~120 for all ions (there are small differences due to the molecular weight). However, for each ion, σ_{1i} is the product of two functions with different peak heights: N_i and $\nu_i/(\nu_i^2 + \omega_i^2)$, so that σ_{1i} peak lies between these maximums. $\nu_i/(\nu_i^2 + \omega_i^2)$ has its peak at almost the same height, ~120 km, for the three ions, it means when $\nu_i \approx \omega_i$. On the other hand, N_i peaks at different heights for each ion species. At noon this peak height is ~105 km for O_2^+, ~130 km for NO^+, and much higher at ~280 km in the case of O^+, where the exact values have a high dependence of season and solar activity level. Consequently, as observed in all panels of Figure 1, σ_{1i} presents its lowest peak for O_2^+, followed by NO^+, and the highest O^+. The conductivity values at each peak decrease rapidly when they occur away from the level where $\nu_i \approx \omega_i$, as can be noticed in the case of O_2^+, and even more clearly in the case of O^+. This is due to the strong decrease of $\nu_i/(\nu_i^2 + \omega_i^2)$ below and above ~120 km, which exceeds the increase of N_i.

The plots on solar maximum activity reveal an interesting increment on the role of O^+ over the conductance, even when the height peak of conductivity is still marked by NO^+, which has a large conductivity in a thin layer, atomic oxygen has a wide conductance layer (Figure 1). Atomic oxygen take even more than 50% of the conductance.

Figure 2 shows the spatial variation of Σ_1 together with each ionic contribution during the equinox month, March, for solar maximum and minimum activity levels at 12 LT. We can clearly notice the Earth's magnetic field effect: higher conductance values are observed where the magnetic field is less intense, corresponding with the South Atlantic Anomaly. At this region the O^+ contribution is greater due to an uplift of the peak conductivity level as a consequence of lower magnetic field intensities which implies a fulfill of the $\nu_i \approx \omega_i$ condition at higher altitudes.

Figure 3 shows the same ionic conductances shown in Figure 2 but as percentage values with respect to the conductance Σ_1. Here in the case of O_2^+ an increase can be noted around the magnetic poles due to a lowering of the peak conducting level as result of greater magnetic field intensities.

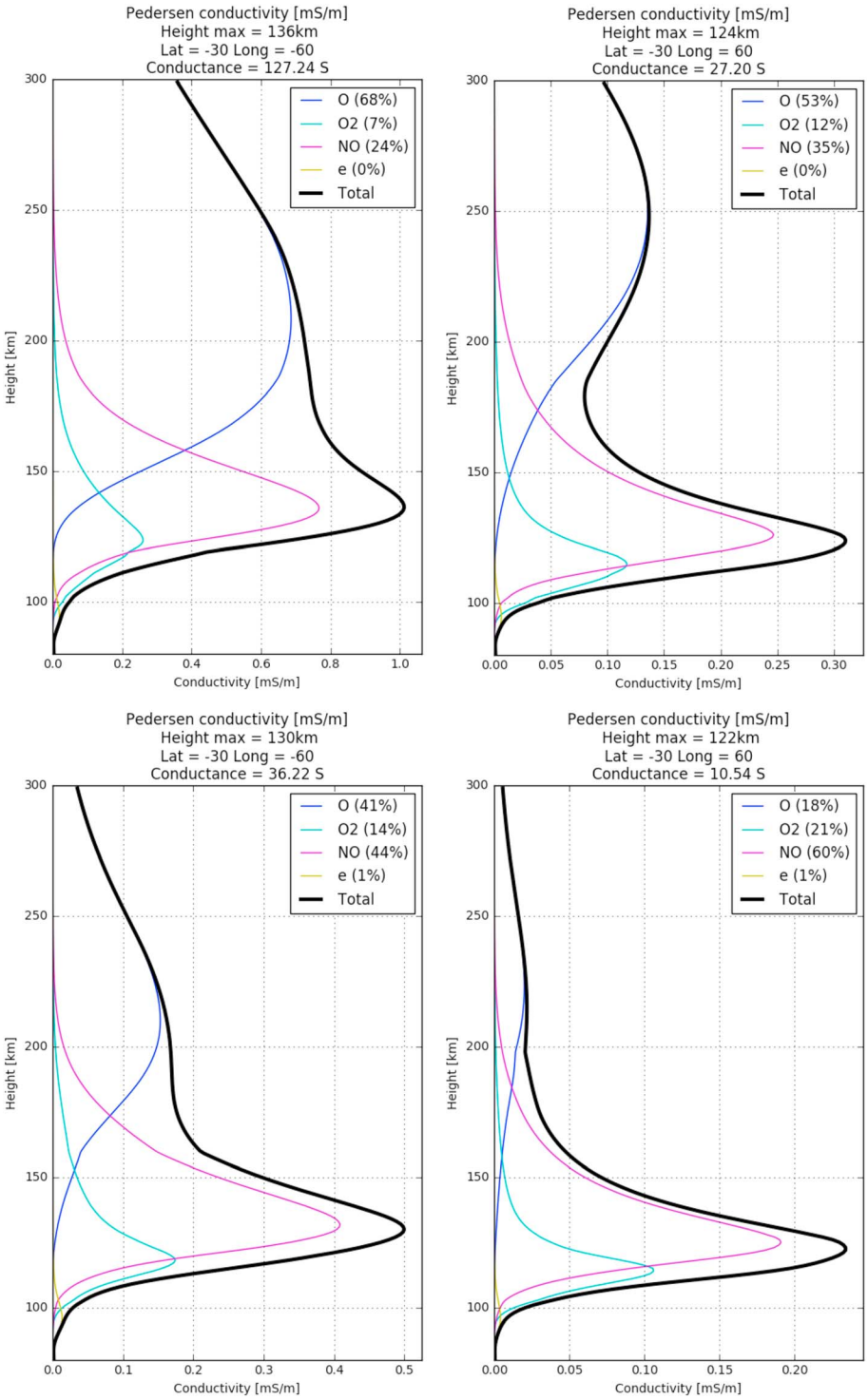

Figure 1. Height profile at 12 LT, for March 2001 (high solar activity level; upper panels) and for March 2008 (minimum solar activity level; lower panels), of Pedersen conductivity, σ_1, each ion contribution: σ_{1NO+} (magenta), σ_{1O2+} (light blue), and σ_{1O+} (blue), and electron contribution: σ_{1e} (yellow), at 30°S, 60°W, which corresponds to a location inside the South Atlantic Anomaly (left panels), and 30°S, 60°E outside the South Atlantic Anomaly (right panels). σ_1 peak height altitude and conductance are indicated at the top of each panel.

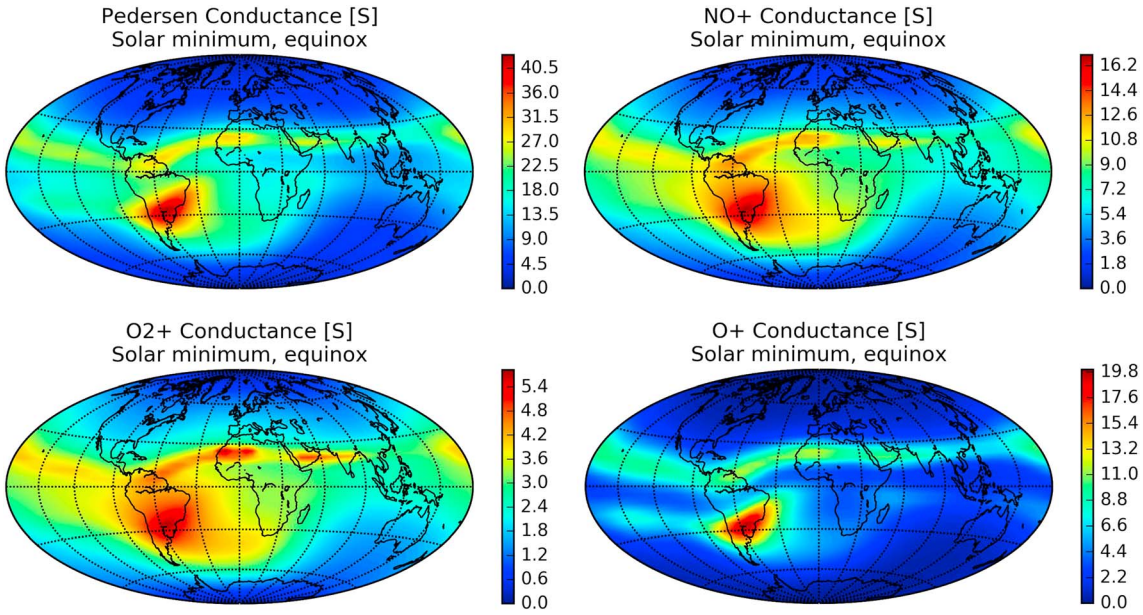

Figure 2. Total Pedersen conductance, Σ_1, and Σ_{1i}, of each ion species for a quiet day equinox month (March) and minimum solar activity level (year 2008).

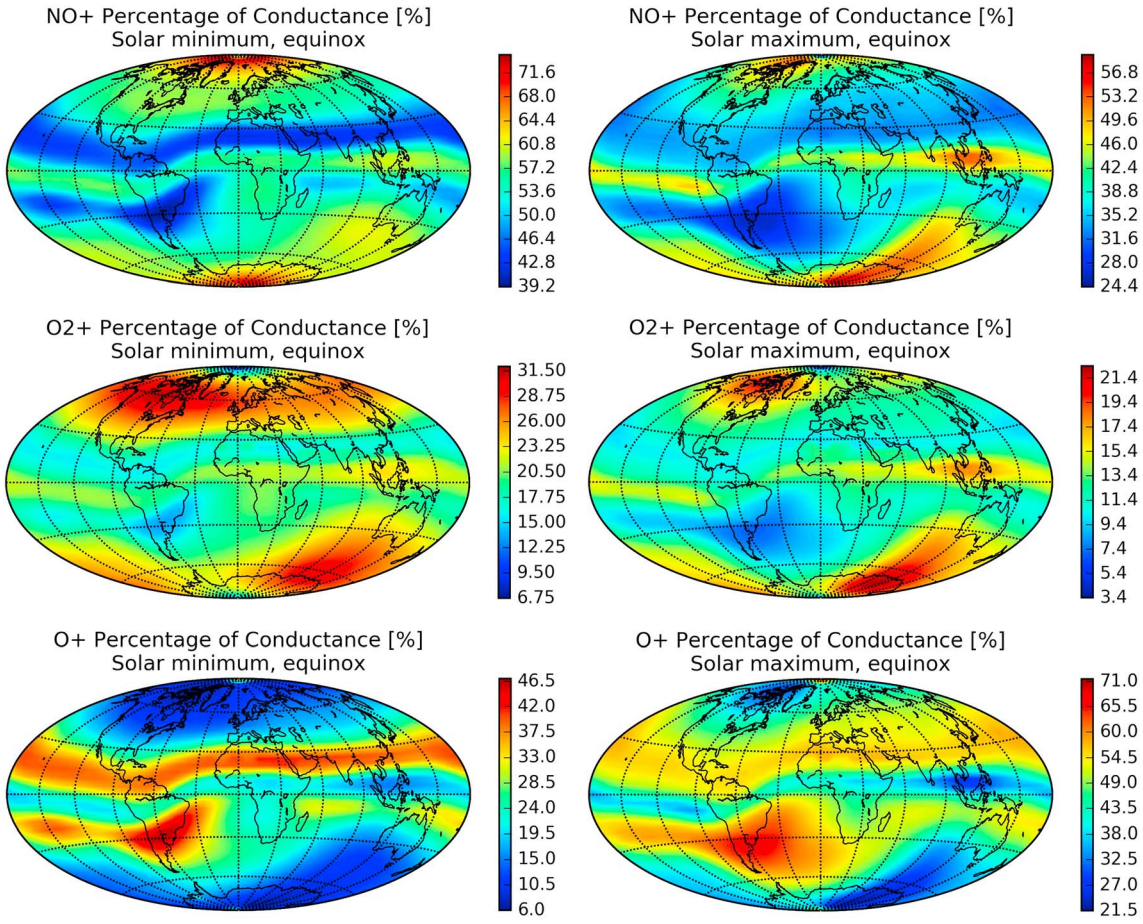

Figure 3. Percent of each ionic Pedersen conductance, Σ_{1i}, relative to Σ_1, at noon for a quiet day equinox month (March) and minimum solar activity level (year 2008; left panels) and maximum solar activity level (year 2001; right panels).

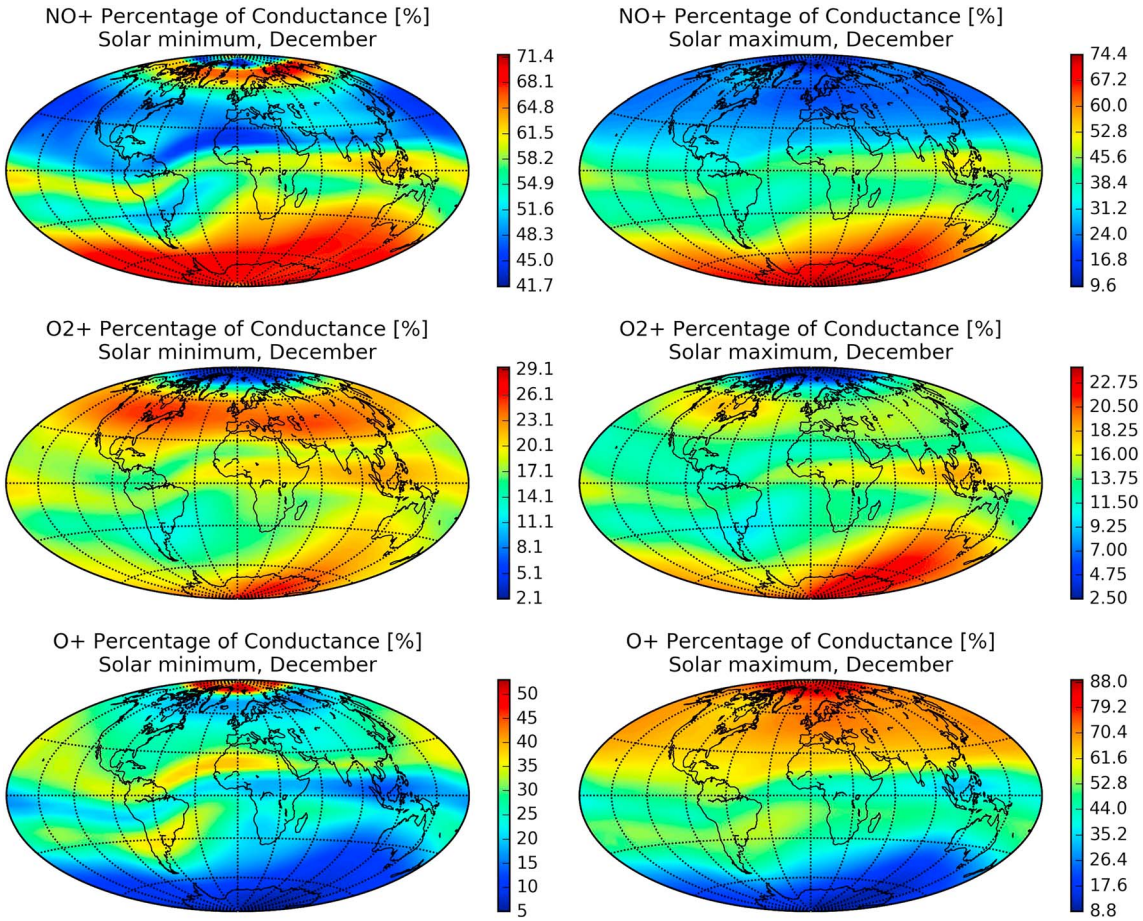

Figure 4. Percent of each ionic Pedersen conductance, Σ_{1i}, relative to Σ_1, at noon for a quiet day solstice month (December) and minimum solar activity level (year 2008; left panels) and maximum solar activity level (year 2001; right panels).

Under minimum solar conditions NO^+ is the principal conducting ion, because represent the highest percentage of conductance in all seasons (Figures 3 and 4). A clear pattern can be seen in the summer hemisphere taking higher values than winter except in the auroral zones. In equinox case, the percentage of NO^+ to conductance shows an evident diminution exactly at south Atlantic magnetic anomaly and the equatorial ionization anomaly where O^+ is deposited due to $E \times B$ effect.

On solar maximum conditions, the spatial structure of conductance of ionic contribution are similar to the solar minimum scenario, with an expected increment on conductance absolute values (not showed). The increase of O^+ contribution, percentage figures, is much greater than that of NO^+. This is because the percentage increase in O^+ density at the *F* layer is higher than NO^+ density at the *E* layer between maximum and minimum conditions. Regions where O^+ contribution exceeds that of NO^+ contribution can be noticed in Figures 3 and 4.

Figure 4 shows the ionic percentage contributions for a solstice month, December. At the north polar region, even though the intense magnetic field, the dominant conducting ion is O^+ due to nighttime conditions which elevates the ionization profile being almost exclusively at the *F* layer, with a nearly absent *E* layer. It can also be noticed the seasonal behavior of NO^+ conductance as a consequence of direct solar ionization being stronger at the summer hemisphere, since the *E* layer is a well behaved Chapman layer.

Percentages for July (not shown) are similar to December but inverted; the summer-winter effect is the more noticeable.

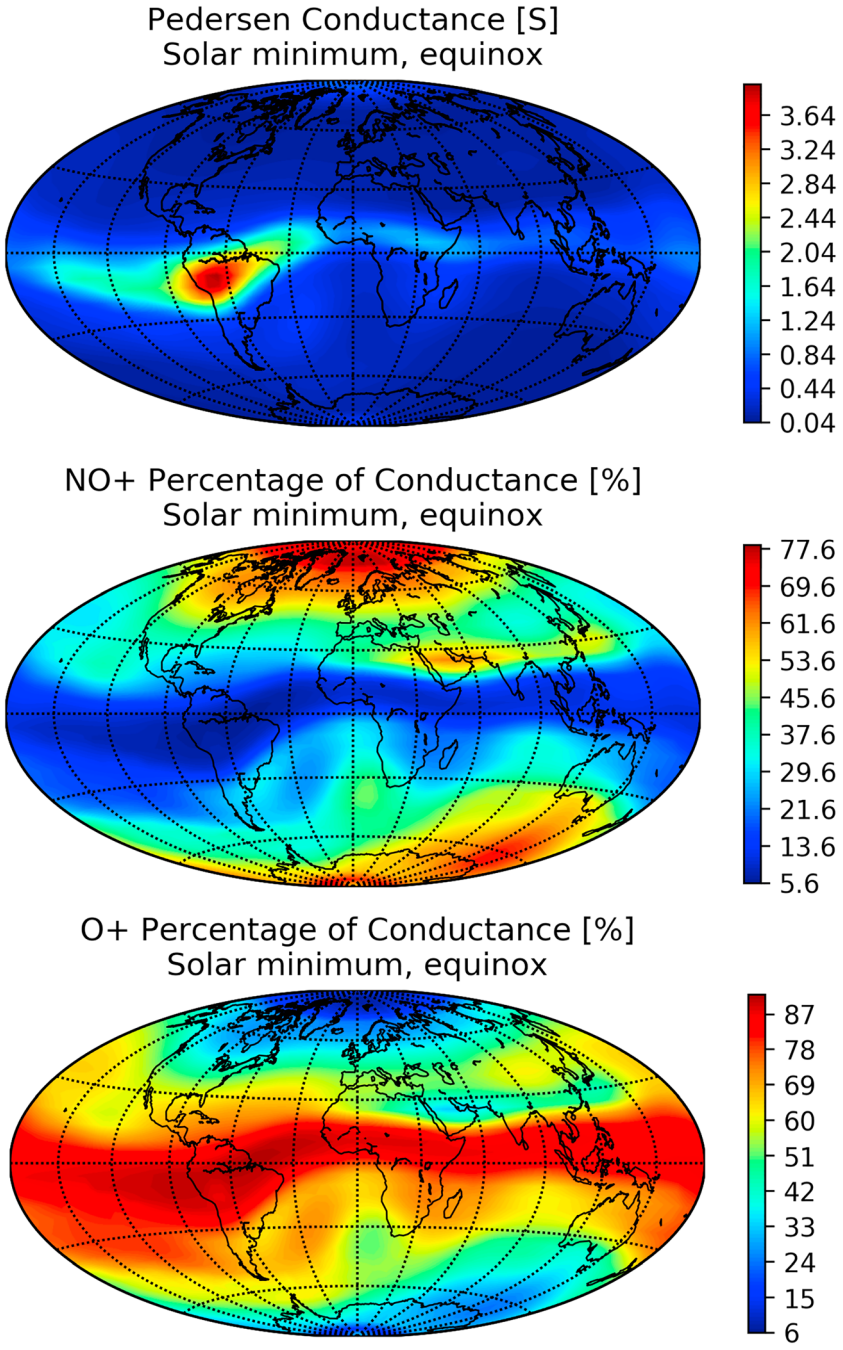

Figure 5. Total Pedersen conductance at 00 LT (top) and percent of NO^+ and O^+, Σ_{1i}, relative to Σ_1, for a quiet day equinox month (March) and minimum solar activity level.

During night, Pedersen conductance presents lower values due to the ions' density decrease. *E* layer's ion density goes almost to zero, and the peak conducting layer moves to the *F* region becoming in this way O^+ the principal conducting ion at low and middle latitudes, as can be noticed in Figure 5, which shows the conductance and the contribution of NO^+ and O^+ at 00 LT. $O_2{}^+$ conductance (not shown) takes globally less than 10%. Near the magnetic poles, the *E* layer take a big percentage of conductance as a result of two effects: high magnetic field intensity that increases conductance at lower heights, and the effect of particle precipitation that enhances ion density at the *E* layer enough to overcome the O^+ conductance.

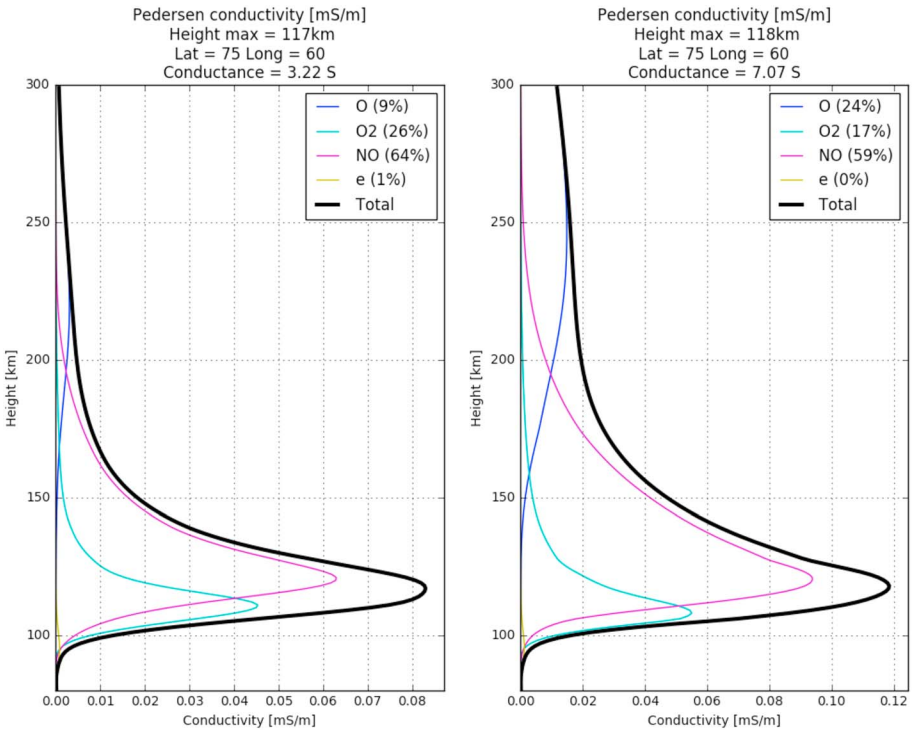

Figure 6. Polar height profile at 12 LT, for March 2008 (left; low solar activity level) and March 2001 (right; high solar activity level) of Pedersen conductivity, σ_1, each ion contribution: σ_{1NO+} (magenta), σ_{1O2+} (light blue), and σ_{1O+} (blue), and electron contribution: σ_{1e} (yellow), at 75°N, 60°W.

4. Conclusions

The conductivity layer is different for each ion. The O^+ peak height is higher than that of NO^+ and O_2^+. It is important then to take this into account since the atomic oxygen, for example, becomes the main conductor at some locations and under certain conditions.

These results are significant for the understanding of energy distribution and ionospheric current system. There are consequences over the simplifications made to simulate or calculate ionospheric properties, for example, considerations as a thin sheet at fixed height, or using only one ion to calculate currents. The energy deposited on polar caps by the vertical currents may depend strongly on the conducting ions in each layer. The carried or transferred by collision energy is not the same for each ion, and neither at the same height.

The height profile in the poles (Figure 6) indicates that the maximum of Pedersen conductivity is near ~115 km and is approximate 60% to NO^+; this is closely related with Joule heating.

The most complex models in the present days, like Thermosphere Ionosphere Electrodynamic General Circulation Model and WACCM-X, calculate the contribution to conductivity of each ion but use it as one total value on calculations, for example, in Joule heating or electron and ion temperature routines.

This article does not intend to change the way that the models work but shows that perhaps we are ignoring some important effects in our treatment of the ionosphere properties. In future works a specific analysis of the effects of every ion to energy budget will be essential to a deeper understanding of the ionosphere.

Acknowledgments
We thank two anonymous reviewers for their comments that have improved this manuscript. We thank ISSI (International Space Science Institute, Bern) and ISSI-BJ (International Space Science Institute, Beijing) for their hospitality and support of the international team on "Climate Change in the Upper Atmosphere" where many ideas in this work were discussed. This work was supported by Projects PICT 2015-0511 and PIUNT E642. Data to calculate conductivities and Earth's magnetic field were freely obtained from IRI-2016 (http://omniweb.gsfc.nasa.gov/vitmo/iri2016_vitmo.html), NRLMSISE-00 (http://ccmc.gsfc.nasa.gov/modelweb/models/nrlmsise00.php), and IGRF (http://omniweb.gsfc.nasa.gov/vitmo/igrf_vitmo.html). This work can be replicated using pyglow, a Python package that wraps several upper atmosphere climatological models. The pyglow package is open-sourced and available at https://github.com/timduly4/pyglow/. The model and simulations are also available from Bruno S. Zossi upon request (brunozossi@hotmail.com).

References

Bilitza, D., Altadill, D., Zhang, Y., Mertens, C., Truhlik, V., Richards, P., et al. (2014). The International Reference Ionosphere 2012—A model of international collaboration. *Journal of Space Weather and Space Climate*, *4*, 1–12. https://doi.org/10.1051/swsc/2014004

Brekke, A., Doupnik, J. R., & Banks, P. M. (1974). Incoherent scatter measurements of *E* region conductivities and currents in the auroral zone. *Journal of Geophysical Research*, *79*(25), 3773–3790. https://doi.org/10.1029/JA079i025p03773

HOA (High Altitude Observatory) (2017). TIEGCM V1.94 Model Description. National Center for Atmospheric Research, Boulder, CO. Retrieved from http://www.hao.ucar.edu/modeling/tgcm/doc/description/model_description.pdf

Moen, J., & Brekke, A. (1990). On the importance of ion composition to conductivities in the auroral ionosphere. *Journal of Geophysical Research*, *95*(A7), 10,687–10,693. https://doi.org/10.1029/JA095iA07p10687

Moen, J., & Brekke, A. (1993). The solar flux influence on quiet time conductances in the auroral ionosphere. *Geophysical Research Letters*, *20*(10), 971–974. https://doi.org/10.1029/92GL02109

Picone, J. M., Hedin, A. E., Drob, D. P., & Aikin, A. C. (2002). NRLMSISE-00 empirical model of the atmosphere: Statistical comparisons and scientific issues. *Journal of Geophysical Research*, *107*(A12), 1468. https://doi.org/10.1029/2002JA009430

Rasmussen, C. E., Schunk, R. W., & Wickwar, V. B. (1988). A Photochemical Equilibrium Model for Ionospheric Conductivity. *Journal of Geophysical Research*, *93*, 9831–9840. https://doi.org/10.1029/JA093iA09p09831

Rishbeth, H., & Garriott, O. K. (1969). *Introduction to ionospheric physics*. New York: Academic Press.

Robinson, R. M., & Vondrak, R. R. (1984). Measurements of *E* region ionization and conductivity produced by solar illumination at high latitudes. *Journal of Geophysical Research*, *89*(A6), 3951–3956. https://doi.org/10.1029/JA089iA06p03951

Schunk, R. W., & Nagy, A. F. (2009). *Ionospheres: Physics, plasma physics, and chemistry*. New York: Cambridge University Press. https://doi.org/10.1017/CBO9780511635342

Sheng, C., Deng, Y., Lu, Y., & Yue, X. (2017). Dependence of Pedersen conductance in the *E* and *F* regions and their ratio on the solar and geomagnetic activities. *Space Weather*, *15*, 484–494. https://doi.org/10.1002/2016SW001486

Strangeway, R. J. (2012). The equivalence of Joule dissipation and frictional heating in the collisional ionosphere. *Journal of Geophysical Research*, *117*, A02310. https://doi.org/10.1029/2011JA017302

Takeda, M., & Araki, T. (1985). Electric conductivity in the ionosphere and nocturnal ionospheric currents. *Journal of Atmospheric and Terrestrial Physics*, *47*(6), 601–609. https://doi.org/10.1016/0021-9169(85)90043-1

Thayer, J. P., Vickrey, J. F., Heelis, R. A., & Gary, J. B. (1995). Interpretation and modeling of the high-latitude electromagnetic energy flux. *Journal of Geophysical Research*, *100*(A10), 19,715–19,728.

Thebault, E., Finlay, C. C., Beggan, C., Alken, P., Aubert, J., Barrois, O., et al. (2015). International Geomagnetic Reference Field: The 12th generation. *Earth, Planets and Space*, *67*(1), 79. https://doi.org/10.1186/s40623-015-0228-9